Title

Selective laser ablation of carious lesions using simultaneous scanned near-IR diode and CO2 lasers

Authors

Chan, Kenneth H
Fried, Daniel

Publication Date

2017-02-08

DOI

10.1117/12.2256696

Peer reviewed

HHS Public Access

Author manuscript

Proc SPIE Int Soc Opt Eng. Author manuscript; available in PMC 2017 June 16.

Published in final edited form as:

Proc SPIE Int Soc Opt Eng. 2017 January 28; 10044: . doi:10.1117/12.2256696.

Selective Laser Ablation of Carious Lesions using Simultaneous Scanned Near-IR Diode and CO_2 Lasers

Kenneth H. Chan and **Daniel Fried**

University of California, San Francisco, San Francisco, CA 94143-0758

Abstract

Previous studies have established that carious lesions can be imaged with high contrast using near-IR wavelengths coincident with high water absorption, namely 1450-nm, without the interference of stains. It has been demonstrated that computer-controlled laser scanning systems utilizing IR lasers operating at high pulse repetition rates can be used for serial imaging and selective removal of caries lesions. In this study, a point-to-point scanning system was developed integrating a 1450-nm diode laser with the CO_2 ablation laser. This approach is advantageous since it does not require an expensive near-IR camera. In this pilot study, we demonstrate the feasibility of a combined NIR and IR laser system for the selective removal of carious lesions.

Keywords

caries removal; near-IR reflectance imaging; selective laser ablation

1. INTRODUCTION

Previous studies have shown that near-IR reflectance imaging beyond 1450-nm is well suited for acquiring high contrast images of occlusal demineralization. [1, 2] This technology holds considerable advantages over conventional caries detection methods, namely it produces images with greater contrast in detecting demineralization from sound tissue, stains do not interfere at near-IR wavelengths, and is non-invasive. [3, 4] In visible reflectance and quantitative light fluorescence, stains often mask demineralization. In the near-IR, the large conjugated molecules associated with stains do not absorb light. Thus, near-IR reflectance is capable of rendering high contrast images of demineralization even in the presence of stains. In combination with computer-controlled laser scanning systems, near-IR reflectance images can be transcribed into ablation maps for precise demineralization removal.

Lasers are well suited for minimally invasive dental hard-tissue treatments. They can achieve precise removal with small laser pulse spot sizes to reach demineralization localized on tooth pits and fissures. CO_2 lasers (λ = 9.3–9.6-μm) have been shown to be well suited for caries removal and has added benefits namely, rendering treated dental hard tissue with higher resistance to further decay.[5] Previous work was done to show that the laser irradiated enamel does not interfere with the ability to image the tooth surface nor significantly distort the contrast between sound and demineralized dental hard tissues.[6] Typical dental lasers are operated by hand, which nullifies their capacity for high precision

and selectivity. Therefore, it is advantageous to employ a computer controlled scanning system to control the laser. High speed scanning systems using micro-electro-mechanical system (MEMS) mirrors and miniature galvanometer based scanners coupled with high repetition rate lasers can reach feasible removal rates. Thus, it is practical to employ a high-speed computer-controlled laser scanning system with a non-invasive caries lesion detection for removing demineralization in a highly conservative manner. Previous studies have demonstrated the feasibility of removing demineralization by sequentially imaging carious teeth with an near-IR InGaAs camera as the CO_2 laser removes the lesion layer by layer.[7, 8]

Previous near-IR reflectance caries removal studies have relied on using expensive InGaAs cameras for imaging, however, lower cost laser diodes and photodetectors are now available at most wavelengths in the near-IR and these can be used with laser scanners to produce similar near-IR images. A point-to-point near-IR scanner can be integrated with a CO_2 laser into a combined real-time image-guided system as a cheaper alternative for selective caries removal. This integrated system is particularly advantageous as it overcomes the challenges of alignment during removal. In this study, we developed an integrated point-to-point scanning system to simultaneously identify and remove caries lesions.

Sample Preparation

Extracted teeth from patients in the San Francisco bay area were collected, cleaned, sterilized with gamma radiation, and stored in a 0.1% thymol solution to preserve tissue hydration and to prevent bacterial growth. Teeth with carious lesions were selected via visual inspection, tactile feedback, and cross-polarized near-infrared reflectance at 1500-nm. Tooth samples were glued down on orthodontic resin blocks for convenience in mounting and scanning.

2.2 Integrated CO_2 Laser and Near-IR Point-to-Point Imaging System

A diagram of the system is shown in Fig. 1. An RF-excited laser, Diamond J5-V from Coherent (Santa Clara, CA) operating at a wavelength of 9.4-μm was used with a pulse duration of 26-μs and a pulse repetition rate of 100-Hz. The laser had a Gaussian output beam. The laser energy output was monitored using a power/energy meter, ED-200 from Gentec (Quebec, Canada). The beam profile was imaged using a Pyrocam Beam profilometer from Ophir-Spiricon (Logan, UT). A room temperature HgCdTe detector Boston Electronics PD-10.6-3 (Boston, MA) with a response time of a few nanoseconds was used to measure the laser pulse temporal profile. The laser beam was focused to a beam diameter of 200-μm using a ZnSe lens of 100-mm focal length. A razor blade was scanned across the beam to determine the diameter ($1/e^2$) of the laser beam. The incident fluence was 30 J/cm^2, which removes ~30-μm of sound enamel per pulse. Computer-controlled XY motion control system ESP-301 and UTM150 stages from Newport (Irvine, CA) were used to create controlled movements of the samples during laser irradiation. A pressure air-actuated fluid spray delivery system consisting of a 780S spray valve, a Valvemate 7040 controller, and a water reservoir from EFD, Inc. (East Providence, RI) was used to provide a uniform spray of fine water mist (5 ml/mm) onto the tooth surfaces.

Linearly polarized and collimated light from a 1468-nm superluminescent diode with a bandwidth of 40-nm and a peak output of 14-mW, Exalos Model 1480 (Langhorne, PA) was combined with the CO_2 laser beam using a beamsplitter and focused with the same 100-mm focal length ZnSe lens onto the occlusal tooth surface. A near-IR InGaAs photodiode detector (Thorlabs, Newton, NJ) was used to collect backscattered near-IR light from the occlusal surface. A near-IR polarizer was placed before the detector to remove specular reflection that interferes with the measurements of the lesion contrast.

2.3 Digital Microscopy

Tooth surfaces were examined after laser irradiation using an optical microscopy–VHX-1000 from Keyence (Elmwood, NJ) with a VH-Z25 magnification lens. Depth composition digital microscopy images (DCDM) were acquired by scanning the image plane of the microscope and reconstructing a depth composition image with all points at optimum focus for displaying a fully focused 2D image. Images of the samples were acquired before and after ablation at 25x.

2.4 PS-OCT System (OCT)

An all-fiber-based optical coherence domain reflectometry (OCDR) system with polarization maintaining (PM) optical fiber, high-speed piezoelectric fiber-stretchers and two balanced InGaAs receivers was designed and fabricated by Optiphase, Inc., Van Nuys, CA. This two-channel system was integrated with a broadband superluminescent diode (SLD) Denselight (Jessup, MD) and a high-speed XY-scanning system (ESP 300 controller and 850G-HS stages, National Instruments, Austin, TX) for rapid *in vitro* optical coherence tomography acquisition. The spectral output of the 15-mW SLD was centered at 1317 nm with a spectral bandwidth full-width at half-maximum (FWHM) of 84 nm. This configuration provided a lateral resolution of approximately 20 μm and an axial resolution of 10 μm in air. The system is described in greater detail in reference [9]. PS-OCT, specifically cross-polarization scans, were used to assess the presence of occlusal lesions and volume of tissue removed by the laser.

2.5 Imaging, Processing, and Caries Removal

A summary of the steps of the algorithm used for removal is shown in Fig. 2. Each step of the algorithm is discussed below. Samples were air-dried for ~20 seconds prior to near-IR point-to-point reflectance image acquisition of the tooth occlusal surface. Images were acquired over an area 10×10-mm with a 50-μm pixel pitch. The backscattered near-IR intensity at each point was averaged over 5 acquisitions to eliminate noisy data. Points were rasterized into a 8-bit near-IR image. Highly scattering demineralized surfaces appear brighter in the near-IR reflectance images, while sound tissues appear dark.

Lesion presence was automatically determined through analysis of the pixel intensity. Image histograms were created and assessed for lesion presence. If the image histogram contained a bimodal distribution of intensities (see Fig. 3 Top left/right), the tooth contained demineralization.

Lesion area was determined through an adaptive thresholding method, which automatically determines an intensity threshold by calculating the median of each peak in the histogram and correlating the distance of each point's intensity to it's respective median within each of the two peaks. A look-up-table (LUT) is created which maps out lesion areas demarcated for laser treatment (see Fig. 4).

Using the acquired LUT, the CO_2 laser was scanned over the identified lesion area for removal. The distance per pulse was roughly ¼ of the spot size diameter of the CO_2 laser. Repeated serial NIR images and LUTs were taken (Fig. 4) until the lesion was no longer determined. Teeth were ablated until the lesion was no longer detected. All image analysis was carried out using Labview (National Instruments, Austin, TX).

2.6 Data Analysis

Teeth were imaged before and after image-guided ablation with PS-OCT and digital microscopy (DCDM). DCDM images were assessed for lesions before ablation and their removal after ablation. Additionally, PS-OCT scans were compared before and after ablation to assay the volume of tissue removed and lesion presence.

3. RESULTS AND DISCUSSION

Serial point-to-point near-IR reflectance images and LUTs of the ablation process are shown in Fig. 4. Demineralization appears with higher intensity than sound enamel in NIR reflectance images. After ten iterations of image-guided removal, demineralization (in white) disappears (Fig. 4F). This demonstrates that the point-to-point scanning approach produces high resolution near-IR images capable of precisely guiding the CO_2 laser and that the laser ablated areas do not interfere with the near-IR point-to-point imaging of enamel.

In addition, 2-D microscopy of occlusal surfaces pre- and post-ablation are shown in Fig. 5 and indicate no sign of thermal or mechanical damage after ablation. Cross-polarized OCT (CP-OCT) data was used to evaluate the lesion volume prior to removal in Fig. 6. Co-polarized OCT data was used to extract geometric surface data before and after ablation. This surface data was then 3D registered using an Iterative Closest Point algorithm to determine the volume of tissue removed (~0.23-mm^3) in Fig. 7. These results indicate that PS-OCT is an invaluable tool for assessing selectivity through quantifying lesion and tissue removal volume.

This study demonstrates the potential of point-to-point near-IR reflectance imaging for image-guided laser ablation of caries lesions within occlusal surfaces. Previous work in selective caries removal relied on operator positioning. In this *in-vitro* study, we used the same scanner for point-to-point imaging and CO_2 laser ablation, which removed alignment/registration error found in non-integrated selective caries ablation systems. Previous work in selective caries removal relied on operator positioning and selecting an optimal threshold for lesion segmentation, however this was not ideal. The robustness of using an adaptive thresholding classifier for lesion detection should allow automatic detection and nonbiased lesion classification.

Although these studies have shown the feasibility of point-to-point near-IR image guided caries ablation, further work is needed to determine the selectivity of image-guided removal. Future studies will involve a larger sample size and appropriate statistics to determine the selectivity of an integrated point-to-point caries removal system. Further work is required to determine if adaptive thresholding can appropriately detect lesion areas by comparing lesion and removal volumes and histology.

Acknowledgments

This work was supported by NIH/NIDCR Grants R01-DE019631 and F31-DE026350.

References

1. Chung S, Fried D, Staninec M, Darling CL. Multispectral near-IR reflectance and transillumination imaging of teeth. Biomed Opt Express. 2011; 2(10):2804–2814. [PubMed: 22025986]
2. Fried WA, Darling CL, Chan K, Fried D. High Contrast Reflectance Imaging of Simulated Lesions on Tooth Occlusal Surfaces at Near-IR Wavelengths. Lasers Surg Med. 2013; 45(8):533–541. [PubMed: 23857066]
3. Bühler CM, Ngaotheppitak P, Fried D. Imaging of occlusal dental caries (decay) with near-IR light at 1310-nm. Optics Express. 2005; 13(2):573–582. [PubMed: 19488387]
4. Almaz, EC., Simon, JC., Fried, D., Darling, CL. Influence of stains on lesion contrast in the pits and fissures of tooth occlusal surfaces from 800–1600-nm. Lasers in Dentistry XXII Proceedings of SPIE; 2016. p. X1-6.
5. Konishi N, Fried D, Featherstone JDB, Staninec M. Inhibition of secondary caries by CO_2 laser treatment. Amer J Dent. 1999; 12(5):213–216. [PubMed: 10649910]
6. LaMantia NR, Tom H, Chan KH, Simon JC, Darling CL, Fried D. High contrast optical imaging methods for image guided laser ablation of dental caries lesions. Lasers in Dentistry XX Proc of SPIE. 2014; 89290:P1–7.
7. Chan KH, Fried D. Selective Removal of Demineralization Using Near Infrared Cross Polarization Reflectance and a Carbon Dioxide Laser. Lasers in Dentistry XVIII Proc of SPIE. 2012; 8208:U1–8.
8. Tom H, Chan KH, Saltiel D, Fried D. Selective removal of demineralized enamel using a CO laser coupled with near-IR reflectance imaging. Lasers in Dentistry XXI Proc of SPIE. 2015; 9306:M1–7.
9. Fried D, Xie J, Shafi S, Featherstone JDB, Breunig T, Lee CQ. Early detection of dental caries and lesion progression with polarization sensitive optical coherence tomography. J Biomed Optics. 2002; 7(4):618–627.

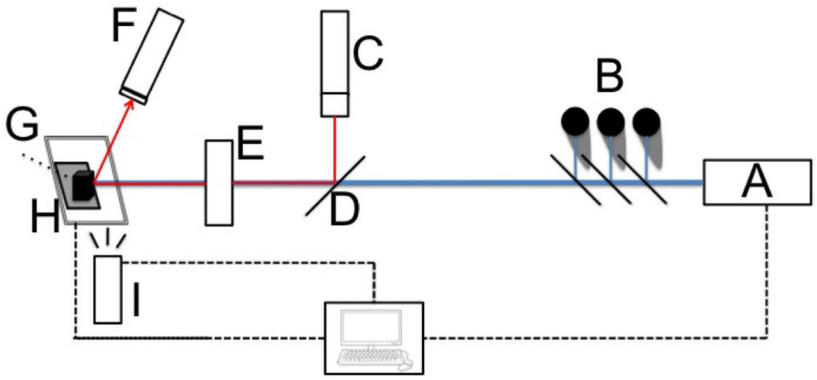

Fig. 1.

Combined point-t0-point near-IR image-guided caries ablation system: (A) CO_2 laser; (B) beam dump; (C) near-IR diode (1450-nm) w/collimator & polarizer; (D) beamsplitter; (E) ZnSe focusing lens; (F) near-IR InGaAs photodiode w/polarizer; (G) tooth sample; (H) XY motion stages; (I) water-/air-spray; (Blue line) CO_2 laser; (Red line) NIR light.

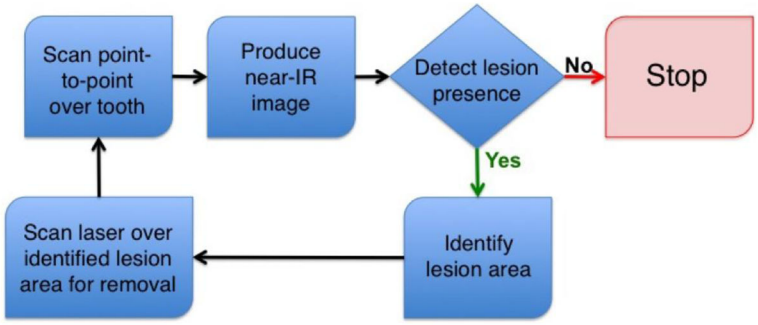

Fig. 2.
Flow-chart of image-guided ablation protocol.

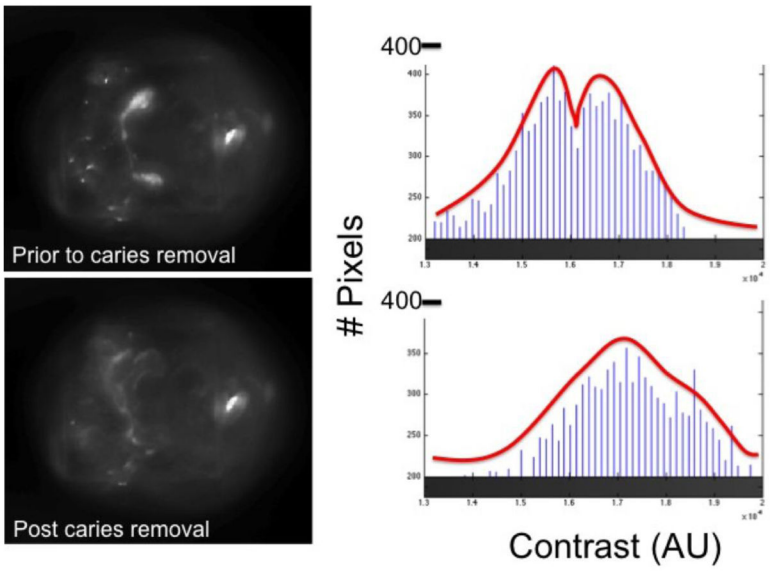

Fig. 3.

Near-IR image and its corresponding image histogram. Note: the red line tracing over the number of pixels at each intensity (AU). Top right: Bimodal peaks shows two distinct intensity distributions within the corresponding image (top left). After selective laser removal (bottom left), the intensity distribution is reduced to a single peak (bottom right). Bimodal intensity distribution indicates lesion presence.

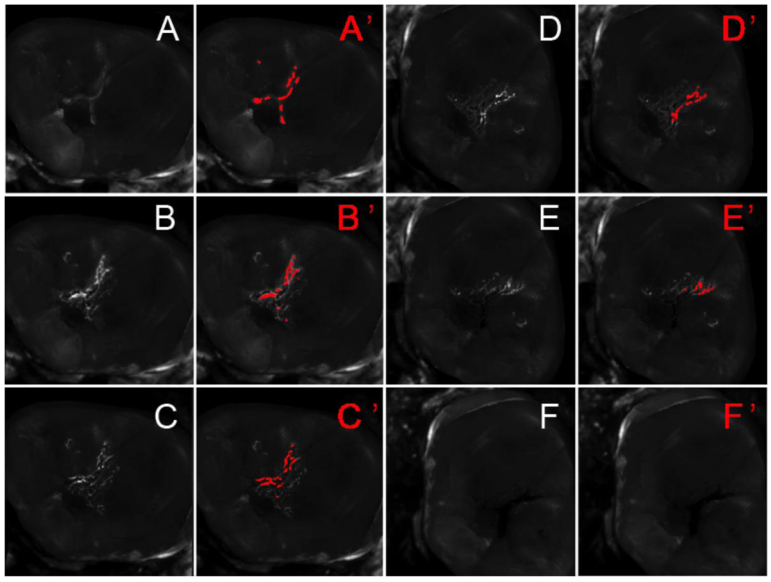

Fig. 4.

(A–F) Left columns, serial near-infrared (NIR) reflectance images acquired after every two iterations. (A′–F′) Right columns, Look-up table (in red) overlaid on top of NIR reflectance images. (A) Initial near-IR point-to-point image of sample. (F) Final near-IR point-to-point reflectance image of sample. After 10 iterations (F), demineralization can no longer be detected, suggesting lesion was completely removed within the pit.

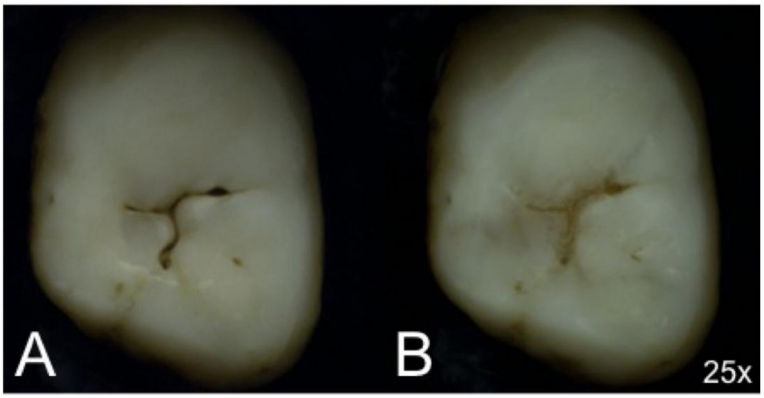

Fig. 5.
Visible reflectance of the tooth sample (A) pre-ablation and (B) post-ablation using digital microscopy. Note: Lack of thermal and mechanical damage.

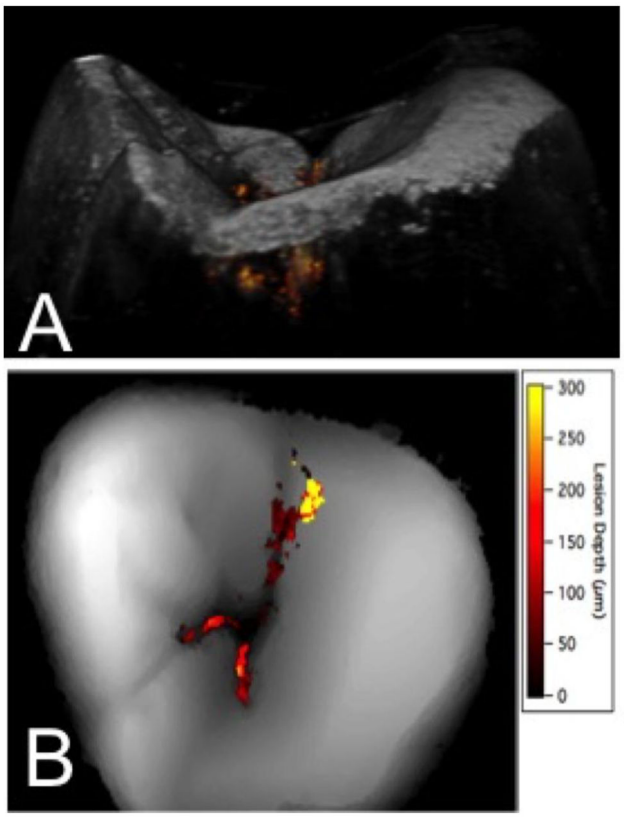

Fig. 6.

PS-OCT visualization of lesion and surface topography (A) 3D tomographic view of lesion (in red/yellow) deep beneath the occlusal surface of the tooth. (B) Surface rendering with lesion depth visualized in colorscale.

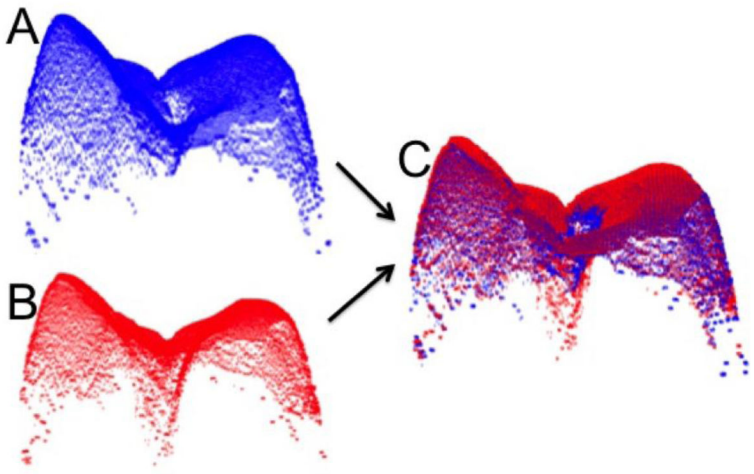

Fig. 7.

3D surfaces imaged with PS-OCT. (A) 3D preablation surface (B) 3D postablation surface (C) Pre-/post-ablation surface 3D registered to determine volume of tissue removed.